Egypt. J. Chem. **Vol. 67**, No. 11 pp. 377 - 399 (2024)

Egyptian Journal of Chemistry

http://ejchem.journals.ekb.eg/

Renewable and Low-cost Agro-waste-based Biosorbents for the Removal of Methylene Blue from water : Analytical Performance and Mechanism Study

Amal AS Al-Yosofy[1], El-Sayed R. H. El-Gharkawy and Magda A Akl[1]*

[1]*Chemistry Department, Faculty of Science, Mansoura University, Mansoura 35516, Egypt*

Abstract

This study presents the utilization of peanut shell agricultural wastes to create environmentally acceptable and cost-efficient biosorbents for the adsorption of cationic methylene blue (MB) dye from water-based solutions. The present study focuses on the production of two biosorbents obtained from peanut shell bio-wastes. The indicated materials comprise unprocessed (SP), as well as sodium hydroxide treated (SPS). The biosorbents undergo analysis using a range of Energy dispersive X-ray spectroscopy (EDX), techniques, such as scanning electron microscopy (SEM), Fourier transform infrared spectroscopy (FT-IR), Brunauer, Emmett and Teller (BET) analysis, N2 adsorption isotherm, X-ray diffraction (XRD), Thermogravimetric analysis (TGA), and determination of the point of zero charge. The batch adsorption approach is employed to determine the ideal operational parameters for removing MB from aqueous solutions. The maximum adsorption capacities were 314.24, and 336.24mg/g for PS, and SPS respectively. The collected kinetics data suggests that the adsorption process of the dye is more accurately characterized by the pseudo-second order model rather than the pseudo-first order model. The equilibrium data exhibited a robust correlation between the dye adsorption and the Langmuir equilibrium isotherm model. An analysis has been conducted on the thermodynamic parameters ΔG°, ΔH°, and ΔS°. The negative standard free energy change (ΔG°) values for both biosorbents demonstrate the inherent spontaneity of the adsorption process. The negative values of ΔH° can explain the exothermic behavior displayed by both biosorbents. The biosorbents derived from peanut shell were efficiently employed for the removal of modest levels of color from different water samples. The adsorption of MB onto SPS is enhanced by many interactions, including pore-filling, electrostatic attraction, π–π, and H-bonding interactions. Methylene blue molecules can diffuse through all the pores of PS, and SPS via pore diffusion

*Keywords***:** peanut shell, sodium hydroxide, methylene blue, wastewater

1. Introduction

The limited availability of drinkable water is a substantial obstacle faced in the contemporary day. The deterioration of water resources is increasingly exacerbating due to various human activities, unregulated urban expansion, and the expanding industrialization[1]. The wastewater generated by various industries contains a variety of contaminants such as dye, heavy metals, antibiotics, and pesticides [2]. Methylene blue dye is a chemical molecule with a planar structure that belongs to the class of heterocyclic aromatic compounds [3]. Methylene blue (MB dye), a regularly used thiazine-type dye, is widely utilized as a colorant in industries including textiles, pharmaceuticals, plastics, tanneries, cosmetics, paper, food, and medicine. Furthermore, it functions as a dye for categorizing microorganisms [4-6]. However, the existence of MB can be a significant threat to the environment and human well-being if not handled appropriately and in an eco-friendly manner [7]. MB dye becomes hazardous to health when its concentration exceeds a particular level, as it possesses significant toxicity [8]. Methylene blue (MB), a substance that is poisonous, carcinogenic, and non-biodegradable, can cause many health risks in humans, such as respiratory failure, abdominal discomfort, visual impairment, and digestive and mental disorders [9,10]. In

*Corresponding author e-mail: magdaakl@yahoo.com .; (Magda A Akl).
Receive Date: 08 January 2024, Revise Date: 22 February 2024, Accept Date: 08 March 2024
DOI: 10.21608/ejchem.2024.258090.9164

addition, it causes symptoms such as nausea, diarrhea, vomiting, cyanosis, shock, gastritis, jaundice, tissue necrosis, and tachycardia, finally leading to cellular apoptosis, tissue damage, and irritation of the skin and eyes [11,12]. Prior to discharging it into the environment, it is imperative to properly treat wastewater that contains MB dye. Various methods and treatment technologies, like as flotation, can be employed to remove MB and other textile dyes from industrial effluent. The techniques mentioned include adsorption, cloud point extraction, photocatalytic degradation, ultrafiltration, electrocoagulation, coagulation, microwave treatment, vacuum membrane distillation, hybrid systems, nanofiltration, and others. Conventional techniques are not successful in breaking down MB dye into smaller inorganic compounds because of its resistance to heat and light, as well as its inability to be broken down by biological processes. Adsorption is commonly recognized as a very efficient method for treating wastewater since it is cost-effective, versatile, and straightforward. Furthermore, adsorption hinders the creation of additional contaminants by means of the oxidation or degrading response of the MB [30, 31]. A wide range of organic and inorganic adsorbents, including zeolites, activated charcoal, clays, chitin, and polymers, are used [32-35]. There is currently a growing interest in using plant residues (agricultural byproducts) to remove colorants. These materials, because of their plentiful occurrence in nature and exceptional ability to remove substances, can be used to absorb colors from solutions that are water-based. Agricultural wastes consist of lignocellulosic materials, which have three main structural components: lignin, cellulose, and hemicelluloses [36]. Lignin is a complex polymer made up of aromatic compounds, which has a highly convoluted three-dimensional structure. The phenylpropane lignin is composed of interlinked chemical units that are linked together by a series of bonds, forming a complex framework that contains various functional groups, such as hydroxyl, methoxy, and carbonyl groups. In addition, hemicellulose is mostly soluble in alkali and undergoes hydrolysis more easily. Lignocellulosic materials consist of both hemicellulose and cellulose, which contain various oxygen functional groups such as hydroxyl, ether, and carbonyl [37]. The presence of these functional groups greatly influences the production process of adsorbents. Literature explores the utilization of different agricultural wastes for the purpose of purifying water and wastewater by eliminating contaminants. Studies have investigated the ability of agricultural wastes, such as sawdust from different trees [38-40], rice hulls [41, 42], leaves from various plants [43-46], seeds [47, 48], fruit hulls [49], peanut shell [50,51]. The substantial production and widespread utilization of peanuts contribute to a significant volume of generated waste. Inadequate management of these byproducts poses a potential threat to environmental pollution, consequently impacting human well-being. Leveraging peanut husk (PH) as an adsorbent for wastewater remediation represents a commendable initiative. This approach is economically viable due to its low cost, environmentally friendly, and aligns with the principles of green chemistry[52].

1.1. Objectives

The aims of the current study can be stated as follows:

1 - Production of SPS mercerized cellulosic biosorbents derived from peanut shell.

2-The structural, surface functional groups, surface potential, textural, and morphological properties of the prepared PS and SPS were analyzed using various instrumental techniques. These techniques included Scanning Electron Microscopy (SEM), Fourier Transform Infrared Spectroscopy (FT-IR), Brunauer, Emmett and Teller (BET) analysis, N2 adsorption isotherm, X-ray Diffraction (XRD), Thermogravimetric Analysis (TGA), and Energy Dispersive X-ray Spectroscopy (EDX).

3 - Investigating the optimal parameters for the absorption of MB dye in water solutions (both in static and dynamic modes) using the developed cellulosic biosorbents. These parameters include pH, contact time, initial MB concentration, biosorbent dosage, and reaction temperature.

4- The experimental data will be examined using several isotherms, such as Langmuir and Freundlich, as well as kinetic model equations, including pseudo-first order and pseudo-second-order.

5 - Examining the desorption experiments with different solvents.

6 - Utilization of the produced biosorbents for the extraction of MB from actual water samples.

7- Investigating the potential mechanism of MB biosorption onto the produced biosorbents.

2. Experimental

2.1 Materials and Method

2.1.1 Materials

The following chemicals were acquired from Sigma-Aldrich: methylene blue dye (MB), hydrochloric acid (HCl), sodium hydroxide (NaOH), sodium bicarbonate (NaHCO3), sodium chloride (NaCl), nitric acid (HNO3), ethanol, and magnesium sulfate (MgSO4). A concentrated solution of MB was created by dissolving the precise quantity of MB in distilled water. The solution was suitably diluted to achieve the intended starting concentration.

2.1.2 Preparation of Adsorbents

2.1.2.1 Preparation of PS adsorbents

The unprocessed outer covering of peanut shell was gathered from the agricultural outskirts of Mansoura,

Egypt. The biowaste materials underwent treatment using 99% ethanol (immersed for a duration of 24 hours), followed by rinsing with distilled water. Ultimately, the biowaste was thoroughly cleansed and then subjected to grinding and sieving processes. After undergoing drying in an oven at a temperature of 75 °C until a stable weight was achieved, fractions measuring between 0.7 and 1.5 mm were chosen.

2.1.2.2 Preparation of SPS biosorbents

The untreated PS was immersed in a solution containing varying amounts of sodium hydroxide (NaOH) at various concentrations (0.1, 0.5, 1, 2, 3, 4, and 5 M) for a duration of 24 hours. This was done to determine the most effective concentration. The biomass of SPS underwent several decantation and filtration procedures. Subsequently, the specimens were thoroughly washed using distilled water until the solutions achieved a neutral pH of 7. Ultimately, they were subjected to a drying process in an oven at a temperature of 75 Ċ until they reached a state of full dryness.

2.2. Instrumentation

The MB dye concentrations were evaluated at the wavelength of maximum absorption (λmax 662 nm) using a Perkin Elmer 550 spectrophotometer. Analyzed utilizing a Jusco instrument (Model 6100, Japan), the FTIR spectra of PS,SPS and SPS-MB were examined. To analyze the physical structure of the materials, we utilized scanning electron microscopy (SEM) with a JSM-T 220A model from JEOL, Japan. The SEM operated at an accelerated voltage of 20 kV.

EDX was utilized for elemental identification by energy-dispersive X-ray analysis. An Oxford X-Max 20 electron microscope, equipped with an EDS detector, was utilized for the experiment.

The surface area was calculated via the Brunauer-Emmett-Teller (BET) equation, which was derived from the N2 adsorption-desorption isotherm data acquired from the BEL SORP MAX instrument manufactured in Japan. The X-ray diffraction (XRD) patterns of the wheat husk and straw samples were obtained using a PANalytical X'Pert PRO diffractometer, which measured the 2-theta (2θ) angle. The thermal stability of the wheat husk and straw materials was evaluated by thermogravimetric analysis (Perkin Elmer TGA 4000) with a heating rate of 15 °C/min, covering a temperature range from 30 to 800 °C.

2.3 Adsorption experiments

2.3.1 Batch adsorption study

In the MB adsorption batch experiments, 0.025 grams of the untreated and altered substances were placed in a conical flask with 25 milliliters of MB solution (50 parts per million) and stirred at a speed of 200 revolutions per minute. The adsorption studies were conducted using a shaker with a constant temperature setting. A comprehensive examination was undertaken to assess the influence of many parameters, such as contact time, dose, initial concentration, ionic strength, temperature, and pH, on the process. The sorption capacity (in mg. g−1) and recovery percentage of MB were determined for the adsorbents using equations 1 and 2, respectively [53].

$$qe = \frac{(Co - Ce)V}{W} \quad (1)$$

$$\%R = \frac{(Co - Ce) \times 100}{Co} \quad (2)$$

The starting concentration of MB solutions is denoted as C_o, whereas the equilibrium concentration is denoted as Ce, both measured in milligrams per gram (mg/g). V represents the volume of the solution containing the adsorbate, measured in liters, while W represents the mass of the adsorbent, measured in grams. %R is the proportion of adsorbates that have been eliminated from the aqueous solution.

2.3.1.1 Studies on point zero charges (pHpzc)

A 0.01 M NaCl solution was created and its pH was measured within the range of 2 to 12 by adding either 0.01 M NaOH or HCl. Afterward, 50 ml of a separate 0.01 M NaCl solution was added, followed by another 0.01 M NaCl solution. Each solution was allocated 1 gram of the corresponding substance. The vials were subjected to incubation for a period of 70 hours, and the final pH of each solution was determined using a pH meter. A comparative graph was created to demonstrate the correlation between the end and starting pH levels [54].

2.3.1.2 Effect of pH

0.025 g of both unaffected and changed materials were added to sealed vials. Each vial contained 25 ml of a dye solution with a starting concentration of 50 ppm for methylene blue (MB). The pH of the solution was initially modified to different values (ranging from 2 to 12) by adding either 0.1 M HCl or 0.1 M NaOH. The sealed bottles containing the solution were then placed in a stable shaker and agitated at a speed of 200 rpm and a temperature of 30 °C for a total of 240 minutes. The absorption studies were conducted under the aforementioned circumstances. The measurement of residual dye was conducted according to the procedures outlined in the Methods section.

2.3.1.3 Effect of dose
To determine the most effective amount of biowaste materials to use as adsorbents, precise quantities of PS and SPS were added to separate bottles with stoppers. Four masses (0.0125 g, 0.025 g, 0.05 g, and 0.1 g) were introduced into hermetically sealed bottles containing 25 mL of the dye solution. The initial concentration of the dye in the MB solution

was 50 parts per million (ppm). The sealed bottles were subsequently placed in a temperature-controlled shaker and agitated for a duration of 240 minutes at ambient temperature at a speed of 200 revolutions per minute. The concentration of the dye in the solid phase at equilibrium (qe) was determined using Equation 1.

2.3.1.4 Effect of initial dye concentration
0.0125 grams of PS, and SPS were introduced into a set of sealed transparent bottles, each holding 25 milliliters of the dye solution. The initial dye concentration was modified to values of 50, 100, 150, and 200 ppm. The sealed transparent bottles were thereafter placed in a temperature-controlled shaker, set at a speed of 200 revolutions per minute, and kept at room temperature for a period of 240 minutes.

2.3.1.5 Isotherms adsorption study
Analyzed the equilibrium isotherm data utilizing the non-linear Langmuir and Freundlich isotherm models. The efficiency of these models was evaluated by applying the non-linear coefficients of determination (R2). The calculations were executed utilizing the Origin software program (version 9). The Langmuir adsorption isotherm states that adsorption takes place at certain uniform spots inside the adsorbent and has been successful in accurately representing several monolayer adsorption processes. The equation for the Langmuir isotherm can be represented as [55]:

$$(Ce)/(qe) = 1/(KL\ qm) + Ce/qm \quad (3)$$

The variables in question are qe, representing the amount of dye adsorbed, qm, representing the maximum adsorption capacity of a monolayer, Ce, representing the equilibrium concentration of the dye in solution, and KL, representing the Langmuir adsorption constant. The Freundlich isotherm is an empirical equation that postulates adsorption taking place on surfaces that are not uniform in nature. The Freundlich equation can be mathematically represented as follows:

$$\ln q_e = \ln KF + 1/n \ln Ce \quad (4)$$

KF and 1/n are adjustable parameters that can be roughly interpreted as the ability and intensity of adsorption, respectively.

2.3.1.6 Effect of the contact time
To do the kinetic experiments, 0.0125g of both PS, and SPS were placed in a set of sealed bottles at various time intervals (30, 60, 90, 120, 150, 180, 210, and 240 minutes). The solution used contained 25 ml of MB dye solution with a concentration of 50 parts per million (ppm) of MB. The preparation is conducted under ideal pH conditions and at room temperature, with constant agitation at 200 revolutions per minute.

2.3.1.7 Adsorption kinetics To determine the step that limits the rate of adsorption, two kinetic models were used to conduct kinetic investigations. The pseudo-first-order kinetic model is represented by the equation [55]:

$$1/qt = Kt/qet + 1/qe \quad (5)$$

The equation that represents the pseudo-second-order kinetics, which is derived from the adsorption equilibrium capacity, can be expressed as:

$$t/qt = 1/(K2q2e) + t/qe \quad (6)$$

The variable qe (mg/g) reflects the degradation efficiency at equilibrium, while qt (mg/g) represents the degradation efficiency at a specific time t (min). K1 corresponds to the rate constant of decay for a pseudo-first-order reaction, whereas K2 corresponds to the rate constant of degradation for a pseudo-second-order reaction. The models k and qe were calibrated together and showed a strong correlation with the experimental deterioration data. The correlation coefficient was utilized to ascertain the optimal kinetic model that precisely correlates to the experimental results.

2.3.1.8 Effect of thermodynamics parameters
The experiment involved the use of multiple airtight bottles, each holding 25 ml of a solution containing 200 parts per million (ppm) of MB at a pH level of 7.5. Within each bottle, a quantity of 0.0125g of both untreated and modified materials underwent agitation for a duration of 240 minutes in a shaker that was pre-stabilized and operated at a speed of 200 rpm. The temperature was consistently kept between 30 and 50 °C. The residual concentration of the dye was determined after adsorption and filtration. The thermodynamic properties energy (Go), enthalpy (Ho), and entropy (So) have been calculated using equations (Eqs. 7) and (Eq. 8) [55]:

$$\Delta Go = -RT \ln Kc$$

$$\ln Kc = (\Delta S°)/R - \Delta H/RT \quad (8)$$

The equation (7) represents the relationship between the change in Gibbs free energy (ΔGo), the gas constant (R), the temperature (T), and the equilibrium constant (Kc).

The gas constant R, which has a value of 8.314 J/mol K, is utilized in the computations. The values of ΔHo were calculated by calculating the slope (−ΔHo/R) of the natural logarithm of Kc versus the reciprocal of temperature (1/T), whereas ΔSo was determined by calculating the intercept (ΔSo/R) of the natural logarithm of Kc versus 1/T.

2.3.1.9 Ionic strength

The impact of different NaCl, NaHCO3, and MgSO4 solutions at concentrations of 0.01, 0.5, and 0.1 M on the adsorption of MB on PS, and SPS samples was examined. The dye concentration was then evaluated after the adsorption and filtration procedure.

2.3.1.10 Desorption studies

Desorption studies were done to evaluate the practical usefulness of biowaste products and cellulose powder. After conducting the biosorption test, 0.05 grams of sorbent with dye were combined with 100 milliliters of 0.1 molar solutions of NaOH, Ethanol, HCl, and HNO3 for desorption. The concentration of dye in the solution was quantified following 120 minutes of agitation. To determine the appropriate eluent, the desorption stages were repeated five times following three concentration tests for the ideal eluent. The desorption of dye by PS and SPS was determined using equation 9 [55].

D%= (amount desorbed to the solution(mg⁄l))/(The amount adsorbed on adsorbents (mg⁄l))*100 (9)

2.3.2 Column studies

Most studies on adsorption columns focused on using artificial wastewater as the substance being adsorbed. In this situation, a solution containing metal or dye is generated and then subjected to treatment with the adsorbent. This work utilized a synthetic MB solution as an adsorbate while employing raw and modified materials as adsorbents. The effects of several process variables, including solution volume, adsorbate flow rate in the column, adsorbent dosage impact, and column diameter, were evaluated using spectrophotometric analysis. Next, the percentage of degradation was calculated using Equation 1. Equation 1 represents the relationship between the dosage impact of adsorbents, while Equation 2 represents the relationship for other factors [55].

2.3.2.1 Effect of dose

PS and SPS were packed in columns with a diameter of 0.7 cm. The materials were dosed at 0.1, 0.15, and 0.2 g. The flow rate of the solution was 0.056 ml/min, and the pH was set at7.5. Additionally, the solution contained 50 ppm of MB.

2.3.2.2 Effect of volume of solution

The experiment involved using different volumes of solution (10, 20, 30 ml) and packing PS and SPS (0.1g) into columns with a diameter of 0.7 cm. The flow rate was set at 0.056 ml/min, the pH was adjusted to 7.5, and the concentration of MB solution was 50 ppm.

2.3.2.3 Effect of column diameter

PS and SPS were placed into columns of varying widths (0.7 and 0.9 cm). The experiment involved applying a flow rate of 0.056 ml/min, a pH of 7.5, a concentration of 50 ppm of MB solution, and a volume of 10 ml of solution, along with 0.1g of each ingredient.

2.3.2.4 Effect of the flow rate

The experiment involved applying PS and SPS at varying flow rates (0.056 and 0.017 ml/min) with a diameter of 0.7 cm. The solution used had a flow rate of 0.056 ml/min, a pH of 7.5, and a concentration of 50 ppm of MB.

3. Results and discussion

3.1. Materials design

3.1.1. Alkali modification of biosorbents

Figure 1 illustrates the alkali modification procedure conducted during a 24-hour timeframe using NaOH solution at different concentrations (0.1, 0.5, 1, 2, 3, 4, and 5). The graphs indicate that the ideal concentration of SPS in the laboratory circumstances was 3 M . All adsorption studies were conducted using the optimal concentration of each substance.

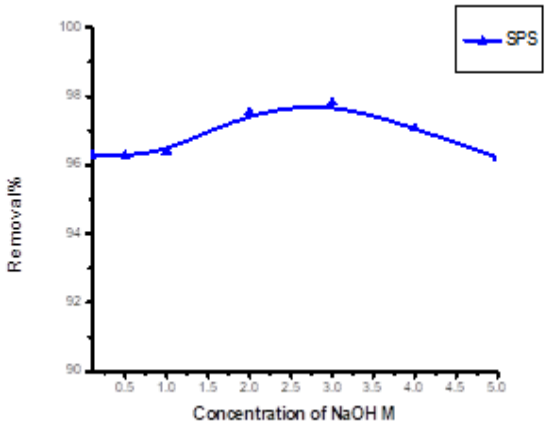

Figure 1: Effect of alkali modification by NaOH at different concentrations

3.1.2. Mechanism of Alkali modification of biosorbents

Applying alkaline agents to PS has been proven to improve their ability to attract and hold substances by (i) removing impurities like waxes and fats from the surface, which exposes chemically reactive functional

groups such as C – OH, C – O, – OH, and C – O; (ii) increasing the capacity for exchanging positively charged ions; (iii) boosting the ability to expand in size; (iv) promoting further expansion; and (v) raising the concentration of oxygenated basic complexes on the surface. Due to its superior disintegrating properties among all alkaline agents, NaOH has been extensively employed for alkaline alteration. The internal arrangement of lignocellulosic components contributes to the formation of a porous structure in the material. The presence of aqueous sodium hydroxide enhances the ionization of the hydroxyl group to form alkoxide in natural fiber [56,57].
on the removal of hemicellulose, scanning electron microscopy images indicate a decrease in hemicellulose content on the surface of the fiber. Figure 2 depicts the FTIR spectra of PS and SPS that have been treatment with an alkaline solution. Second.

3.2 Characterization

3.2.1 FTIR analysis

Figure (2) presents the FTIR spectrum of the materials in three states: before treatment with sodium hydroxide, after treatment with sodium hydroxide, and after the adsorption of MB dye. To elucidate the specific functional group that exists on the surface of the adsorbent. A total of 400 milligrams of KBr were utilized to encapsulate SP, and SPS before the adsorption process. Subsequently, SPS was encapsulated again following the adsorption of MB dye. This procedure was conducted to detect infrared spectra. The spectra were obtained using a Fourier Transform Infrared (FTIR) instrument, covering a wavelength range of 500 – 4,000 cm-1.
The FTIR spectra of untreated samples (PS), NaOH-treated sample (SPS), and NaOH-treated sample after the methylene blue dye adsorption process were analyzed. The results demonstrate that (PS) without NaOH treatment display a –OH functional group within the wavenumber range of 3451 cm^{-1}. These wavenumbers correspond to the anticipated stretching of the –OH group, which typically occurs between 3100 and 3600 cm^{-1}. This observation suggests the existence of phenol, alcohol, and water groups. The detected functional groups originate from cellulose, hemicellulose, and lignin, accompanied by C-H stretching at wavenumbers of 2925 cm^{-1} for PS, Cellulose and hemicellulose are responsible for the C–H stretching seen in the range of 2500 to 3000 cm^{-1} [58, 59].
After subjecting the substance to alkali treatment using NaOH, there is an observable change in the wavenumbers to 3419 cm^{-1} for PS. This shift indicates the elimination of lignin content, which commonly contains a -OH group. The purpose of NaOH treatment is to remove lignin, hemicellulose, and other contaminants. Furthermore, the lack of hemicellulose impurities is indicated by the absence of wavenumbers associated with the carbonyl group (C=O) at 1633-1659 cm^{-1} for SPS [60,61]. The presence of functional groups such as -CH, -OH, and CH2 bending, indicating hemicellulose content, is observed in all four samples within the wavenumber range of 1500 to 1000. The application of chemical treatment diminishes the amplitude of the wave, indicating a reduction in hemicellulose content on the surface of the material. While the FTIR plot does not explicitly demonstrate the impact of alkali treatment

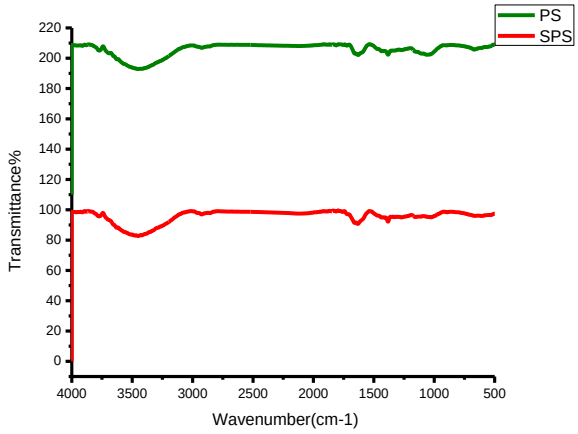

Figure 2: FTIR spectra of PS and SPS.

3.2.2 Scanning electron microscopy (SEM)

Scanning electron microscopy (SEM) is a technique used to examine samples at high resolution by using a focused beam of electrons to scan the surface of the sample. The morphology of PS and SPS is investigated using scanning electron microscopy. The surface shown in Figure 3 is characterized by its morphology. The impact of the sodium hydroxide modification is evident when comparing the images of the original materials and their altered versions. Compared to PS surfaces, SPS surfaces exhibit greater irregularity and porosity, resulting in an increased specific surface area. This enhancement in structure contributes to their higher adsorption capabilities.

3.2.3 Thermogravimetric analysis

The TGA curves of PS and SPS were shown in Figure (6), the samples show an initial weight loss ranging from 70 to 250 °C, and 90 to 200 °C for PS and SPS respectively, which would be related to the evaporation of the adsorbed water molecules in both PS and SPS degradation [67]. The second weight loss gradually starts with a sharp fall at 270 to 380 °C, and 270 to 360 °C for PS and SPS respectively,

this would correspond to the degradation of the impurities content of PS and SPS degradation [53]. The thermal degradation was studied under the same conditions for S and SPS the total residues were determined as follows 18.5%, and 28.8% for PS, SPS respectively. PS showed higher weight losses than SPS, which is due alkali treatment reducing the cementing material followed by the removal of moisture, which makes the treated fiber more stable than the untreated fiber [68,69].

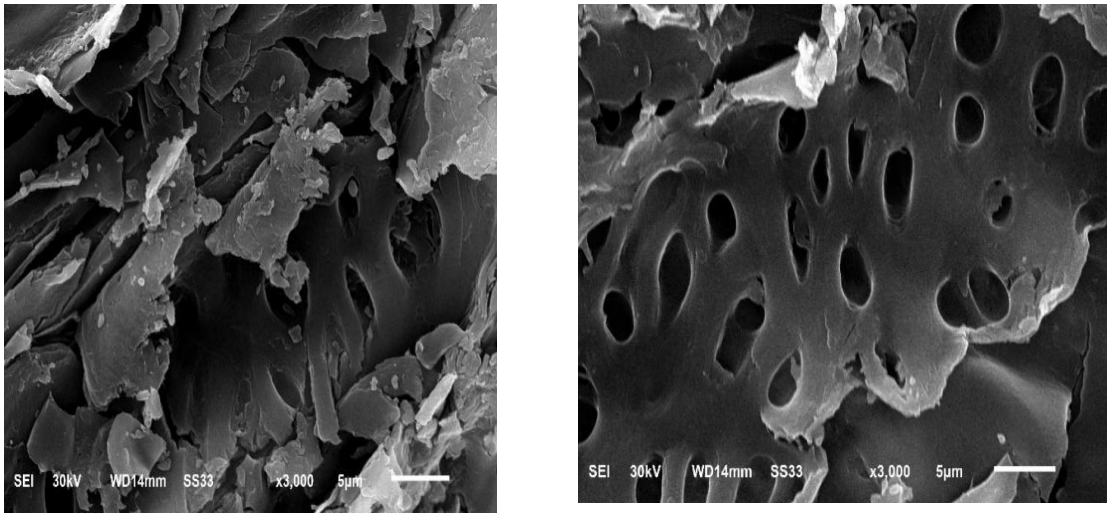

Figure: 3 SEM photographs of **(a) PS, (b) SPS**

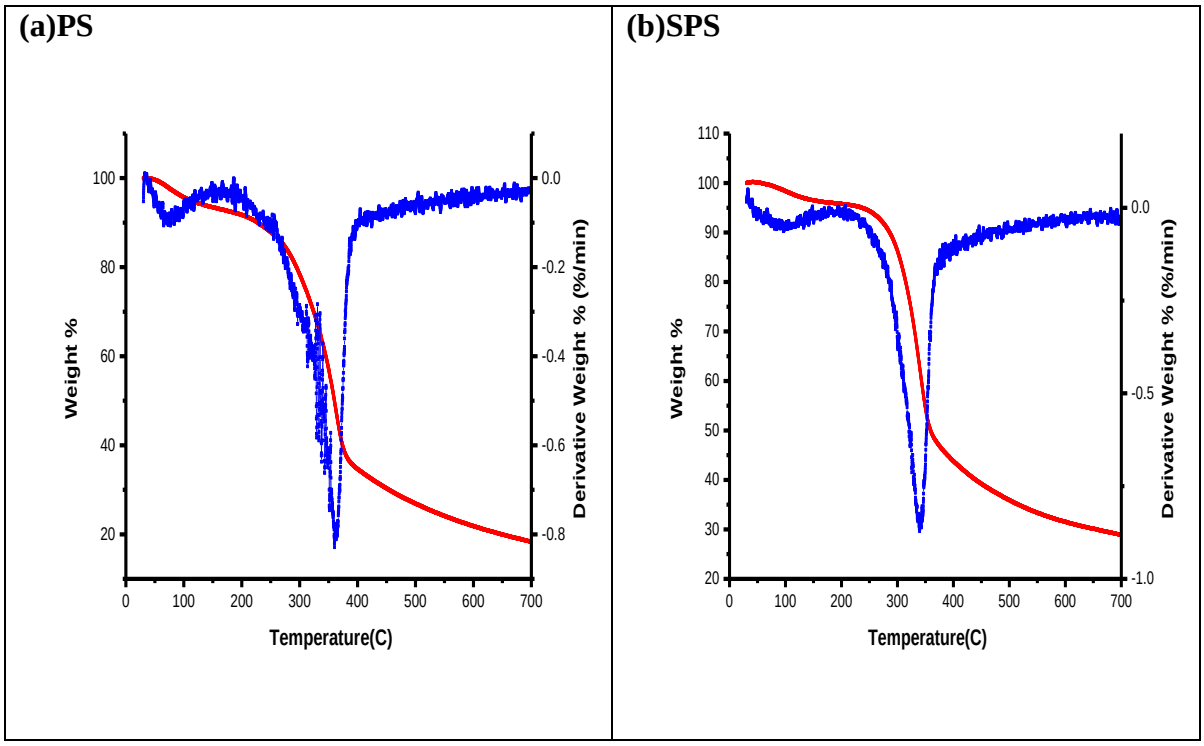

Figure 4: TGA of (a) PS and (b)SPS.

3.3.3 Adsorption studies

3.3.1 Point of zero charges (pH_{pzc})

The point of zero charges (pHpzc) is an important factor that determines the linear range of pH sensitivity and then indicates the type of surface-active centers and the adsorption ability of the surface. Many researchers studied the point of zero charges of adsorbents that are prepared from agricultural solid wastes in order to better understand of adsorption mechanism. Cationic dye adsorption is favored at pH>pHpzc, due to the presence of functional groups such as OH-, and COO- groups. Anionic dye adsorption is favored at pH<pHpzc where the surface becomes positively charged [70] . The pH_{PZC} was shown in Table (1) for materials before and after sodium hydroxide modification which determines the charge on the surface present as mentioned.

Table 1. pH_{PZC} for PS, and SPS.

materials	pH_{PZC}
PS	6
SPS	7.11

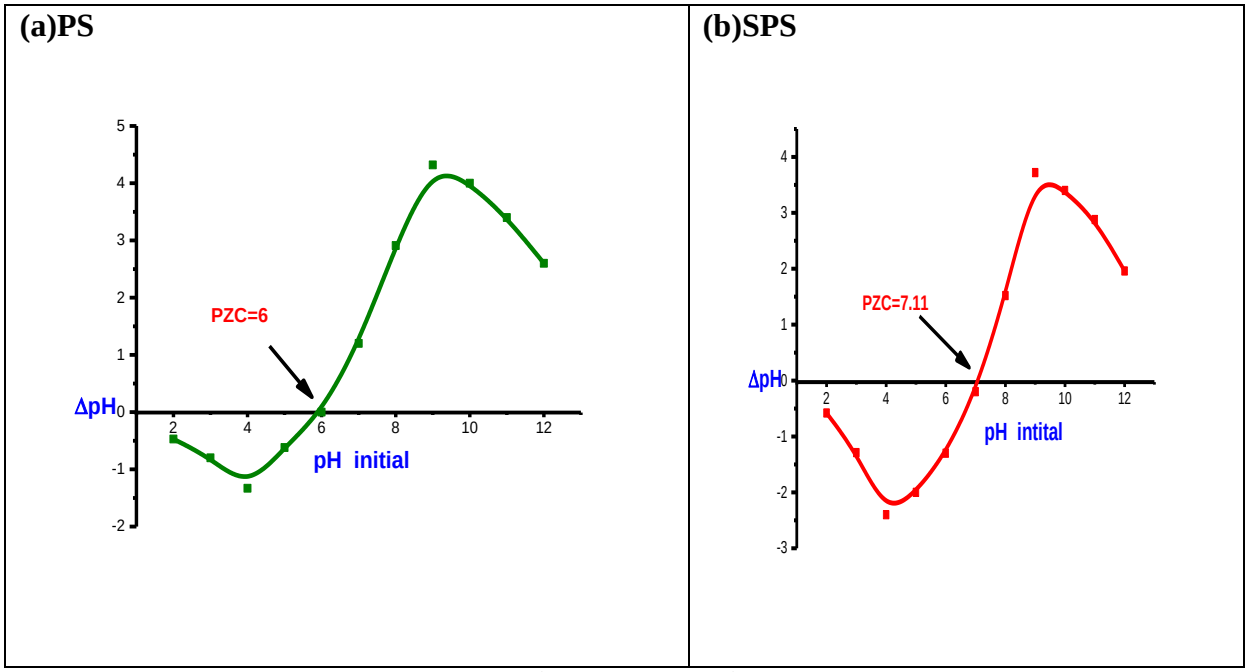

Figure 5: Point of zero charge (pH_{pzc}) of (a)PS (b)SPSP.

3.3.2 Effect of pH on MB adsorption

Figure 8 illustrates the impact of pH on the adsorption of Methylene Blue (MB). The observed data indicates that pH plays a significant role in influencing the adsorption process, particularly for MB, which is a cationic dye existing in an aqueous solution as positively charged ions (MB+). The degree of adsorption onto the adsorbent surface is predominantly governed by the surface charge on the adsorbent, which, in turn, is contingent upon the solution pH. As depicted in Figure 4, the removal percentage exhibited a minimum at pH 2 (3.58% and 18.7%) for Pr and Pm, respectively. Subsequently, the curves exhibited an increase up to pH 6 and 7, followed by a near-constant removal percentage (90%) for PS and SPS within the initial pH range of 7-12 at a concentration of 50 ppm.This observed phenomenon is attributed to the presence of excess H+ ions in the adsorbate, competing with the cation groups on the dye for adsorption sites The lower adsorption of MB at acidic pH (pH < pHpzc) is a result of the abundance of H+ ions, which hinder the adsorption of cationic dye molecules. Conversely, at higher solution pH (pH > pHpzc), Pr and Pm are likely negatively charged, facilitating electrostatic attraction with the positively charged dye cations, leading to enhanced adsorption. This finding aligns

with a similar result reported by Do et al. (2021), where the adsorption percentage of MB increased from 94.60% to 97.50% as the pH of the solution rose from 4 to 11[71]. This underscores the crucial role of pH in modulating the electrostatic interactions and, consequently, the adsorption behavior of cationic dyes onto modified adsorbent surfaces. All of the following experiments were validated at pH 7.5.

3.3.3 Effect of adsorbent dose

Adsorbent dosage is a critical factor that has a substantial impact on the adsorption process, influencing the adsorbent's capacity for adsorption. In Figure 9, variations in dosage for the adsorption of Methylene Blue (MB) at various masses are depicted. It is evident across all materials that the adsorption capacity decreases as the adsorbent dose increases. The reduction in sorption capacity with an increasing dosage of adsorbent at a constant dye concentration and volume can be attributed to the saturation of adsorption sites caused by particle interactions, such as aggregation. The aggregation phenomenon leads to a decrease in the total surface area of the adsorbent and an increase in the diffusional path length. Consequently, as the adsorbent dose rises, the available surface area for adsorption diminishes, and the diffusion of dye molecules to active sites becomes less efficient. To address this issue and maintain a consistent and effective adsorption process, the adsorbent dose for subsequent studies was set at 0.0125 g/25 ml. This optimized dosage aims to balance the need for a sufficient quantity of adsorbent for effective adsorption while avoiding excessive dosages that may lead to reduced adsorption capacity due to particle aggregation and diminished accessible surface area

3.3.4 Effect of initial concentration on MB adsorption

Figure 10 illustrates variations in the initial dye concentration during the adsorption process of Methylene Blue (MB) at different concentrations. A noticeable trend is observed wherein the adsorption capacities increase for both adsorbents as the initial concentrations of MB rise. This phenomenon can be attributed to the saturation of active sites available for the set adsorbent dose. At lower initial concentrations of MB (50 ppm), only a few adsorbent molecules occupy the adsorbent's surface, resulting in a decline in the adsorption capacity of MB. In contrast, an increase in the initial MB concentration to 200 ppm leads to a higher coverage of the adsorbent surface by MB molecules, causing a corresponding increase in the adsorption capacity of MB. To ensure consistent and effective adsorption conditions in subsequent experiments, the initial dye concentration was standardized and fixed at 200 ppm. This concentration was chosen to strike a balance, avoiding the limitations observed at lower concentrations while preventing excessive saturation of active sites at higher concentrations. By setting the initial dye concentration at 200 ppm, the study aims to maintain optimal conditions for adsorption and provide reliable insights into the adsorption behavior of MB on the specified adsorbents

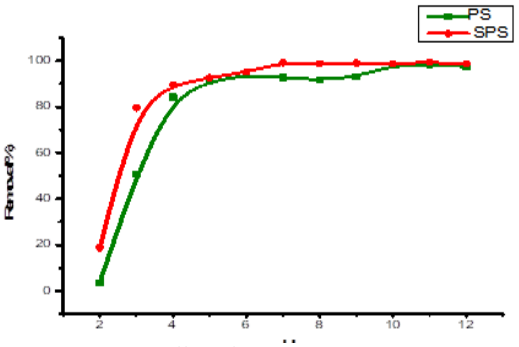

Figure: 6 Effect of pH on the adsorption o

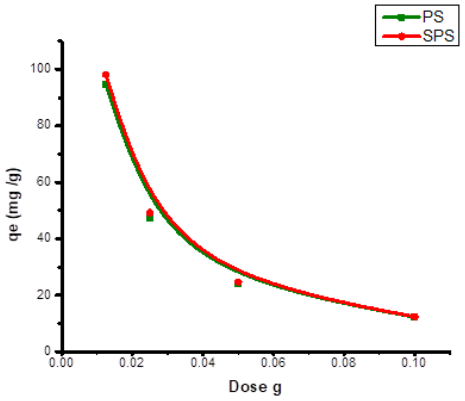

Figure 7: Effect of sorbents dose in the adsorption of MB (PS, and SPS).

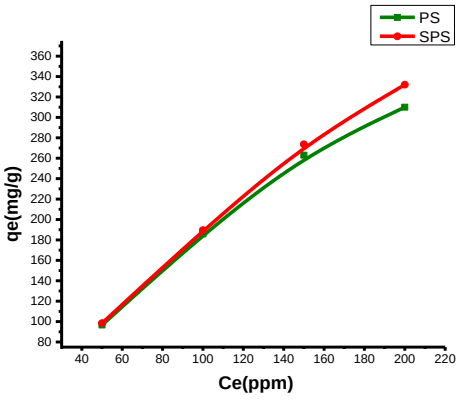

Figure 8: Effect of initial dye concentration in the adsorption of MB.

3.3.5 Adsorption isotherms

The adsorption capacity of an adsorbent is commonly predicted through isotherm studies. In this study, nonlinear Langmuir and Freundlich isothermal equations, represented by Eqs. (5) and (6), were utilized to analyze the experimental Methylene Blue (MB) adsorption data at equilibrium conditions. The corresponding plots are presented in Figure 11. The Langmuir isotherm assumes the formation of monolayers at homogeneous sites. Table 2 displays the calculated parameters of Langmuir Isotherms, revealing a maximum adsorption capacity of 344.83 mg/g and 363.64 mg/g for PS and SPS, respectively. The Langmuir constant (KL) was further employed to assess the separation factor (r). A value of r between 0 and 1 suggests favorable adsorption; in this case, the calculated r values fell within this range, indicating favorable adsorption. The values of r provide insight into the nature of adsorption: if r > 1, adsorption is unfavorable; if r = 1, it is linear; if 0 < r < 1, it is favorable; and if r = 0, it is considered irreversible.

On the other hand, the Freundlich isotherm assumes a heterogeneous distribution of adsorption sites. The calculated KF values were 84.83 and 108.69 for PS and SPS, respectively. The determination coefficient (R2) was used to compare the fit of the Langmuir and Freundlich models. In both cases PS and SPS), the Langmuir isotherm was found to be preferred over the Freundlich isotherm, as indicated by higher R2 values. In summary, the Langmuir model suggests the formation of monolayers at homogeneous sites, and the favorable adsorption indicated by the separation factor (r) is consistent with the calculated parameters for both PS and SPS. The results support the conclusion that the Langmuir isotherm provides a better fit to the experimental data in comparison to the Freundlich isotherm.

capacity was 280.11, and 290.69 (mg/g) for CP, and SCP respectively. The K_L value was further used to evaluate the separation factor (r). If r > l adsorption is unfavorable, r = l it is linear, 0 < r < l it is favorable, and if r = 0, it is irreversible. In both cases, the calculated value of r was between 0 and 1, suggesting favorable adsorption Freundlich isotherm assumes heterogeneous distribution of adsorption sites. K_F values were 51.64, and 59.21 for CP, and SCP respectively. The R^2 indicates that in both cases (CP, and SCP) Langmuir is preferred over Freundlich.

Table 2. Langmuir and Freundlich isotherms constants for adsorption of Methylene blue dye

Sample	Langmuir constants			Freundlich constants		
	qm(mg/g)	K_2 (L/mg)	R^2	K_f	n	R^2
PS	344.83	0.00312	0.997	84.83	2.759	0.962
SPS	363.64	0.2781	0.990	108.69	3.01	0.986

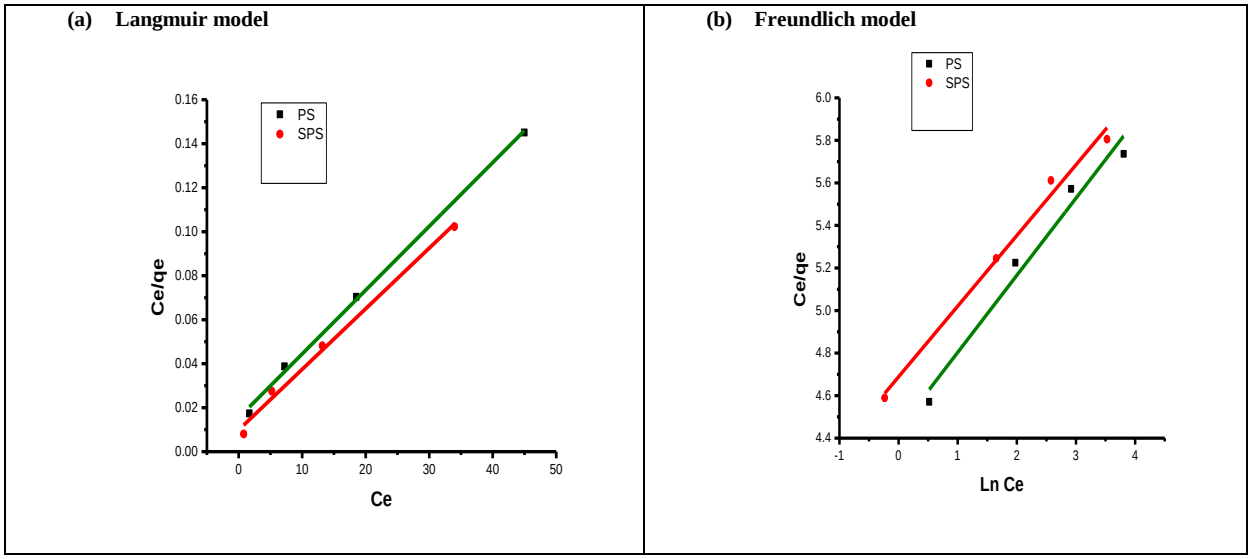

Figure 9: Adsorption isotherm Langmuir model (a)and Freundlich(b) for MB.

3.3.6. Effect of contact time.

In order to determine the optimal duration required to achieve equilibrium, the impact of contact time on the adsorption process of MB was examined at different intervals. Figure 12 illustrates the impact of interaction time on the outcomes. The proportion of MB removal increased as the period of contact between the MB and the adsorbents increased, reaching equilibrium after approximately 175 minutes. After reaching a state of equilibrium, the quantity of adsorbed MB remains rather constant over time without any significant fluctuations. From the provided figure, it is evident that the adsorption process exhibits a rapid starting rate (75 minutes). This phenomenon can be attributed to the presence of several active sites on the adsorbent material during the initial stage. This resulted in an elevation of concentration gradients between the initial adsorbate in the solution and the initial adsorbate on the adsorbent surface. Over time, the concentration diminishes due to the influx of additional MB particles occupying the vacant sites. This leads to a deceleration in the rate of adsorption, heightened saturation of active sites, and eventual occupation of all exchange sites. The optimal duration for the succeeding studies was 180 minutes.

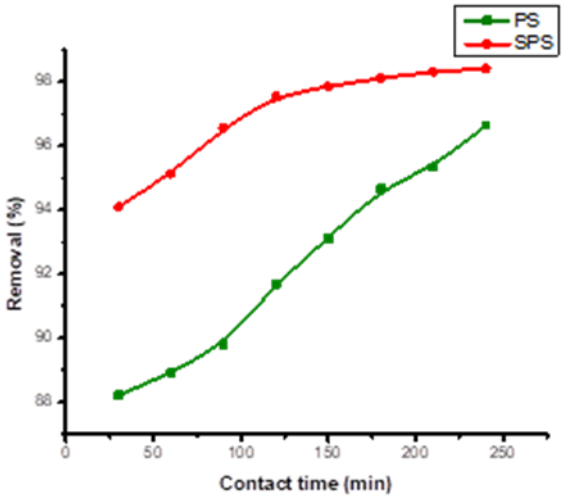

Figure 10: Effect of contact time on the adsorption of MB.

3.3.7 kinetic adsorption study

The dynamics of adsorption can be elucidated by studying the kinetics of the process, particularly focusing on the order of the rate constant. This parameter is crucial in selecting suitable materials for adsorption applications, as an effective adsorbent should not only possess a large adsorption capacity but also exhibit a fast adsorption rate. Pseudo-first-order and pseudo-second-order models are commonly employed to investigate adsorption kinetics. The pseudo-first-order model posits that the adsorption rate is proportional to the first power of concentration, characterizing the process as diffusion through a boundary. However, this model may not always fit well for the entire range of contact time, leading to deviations from theoretical predictions. In such cases, the pseudo-second-order model is often utilized, assuming that chemisorption is the rate-controlling step in the adsorption process. In the analysis of the transient behavior of Methylene Blue (MB) adsorption by PS and SPS, both pseudo-first and pseudo-second-order kinetic models were employed, and the results are depicted in Figure 13. The rate constants (k1) derived from these plots, along with the corresponding correlation coefficients, are presented in Table 3. The selection of the best-fit model is typically based on the linear regression correlation coefficient (R2) values. For cationic dye adsorption, the pseudo-second-order model generally provides a better representation of kinetic adsorption. The R2 values for the pseudo-first-order kinetic model ranged from 0.613 to 0.889, indicating a less satisfactory fit. Conversely, the R2 values for the pseudo-second-order model were close to 1, surpassing the R2 values obtained for the pseudo-first-order model. Therefore, the adsorption kinetics of MB on PS and SPS are more accurately and favorably described by the pseudo-second-order kinetic model

.

Table 3. First and Second – order kinetic equation for adsorption of Methylene blue dye

Sample	First – order kinetic equation			Second – order kinetic equation		
	qe(mg/g)	K_1 (L/min)	R^2	qe(mg/g)	K_2 (g/mg.min)	R^2
CP	171.81	1.9107	0.954	89.93	0.019351	0.999
SCP	115.61	1.2821	0.926	90.33	0.01155	0.999

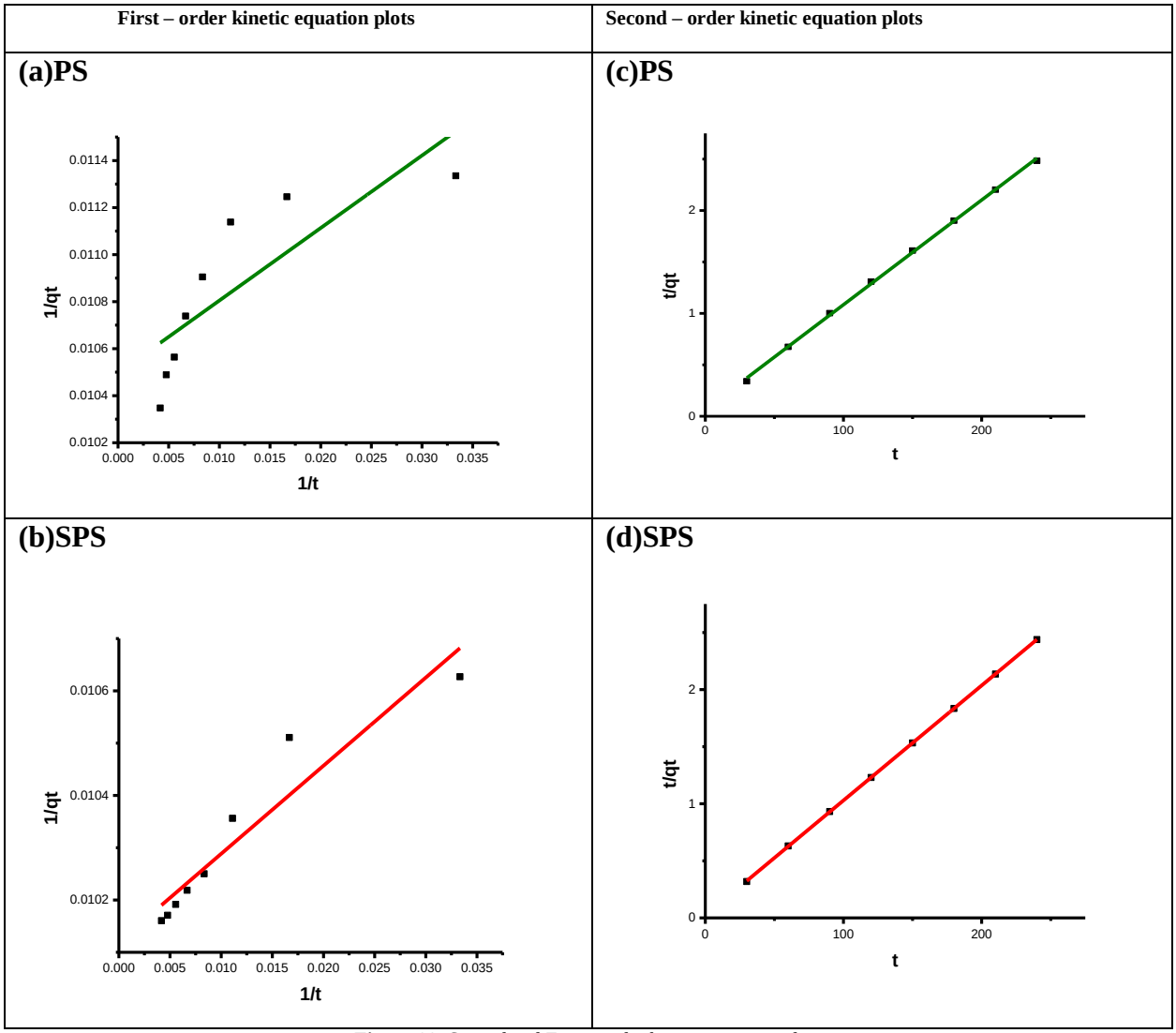

Figure 11: Second and First – order kinetic equation plots

3.3.8 Effect of temperature and thermodynamics parameters

3.3.8.1 Effect of temperature.

The significance of adsorption is influenced by temperature fluctuations. Additionally, it discloses whether the process is endothermic or exothermic. The studies were conducted at three distinct temperatures, specifically 303, 313, and 323 K, while keeping the other parameters unchanged. The percentages of dye elimination for PS, and SPS at 303 K were 78.56%, and 84.06% respectively. These percentages fell to 76.21%, and 82.11% at

323 K. The removal rate dropped as the temperature increased, indicating that the adsorption process was exothermic in both cases.

3.4.8.2 Thermodynamics

Thermodynamic properties such as enthalpy, entropy, and Gibbs free energy have all been investigated. Table 4 and Figure 14 display the thermodynamic parameter values determined for the present system. The standard Gibbs free energy (G°) values for the removal of methylene blue on PS, and SPS were determined to be negative, indicating that the process is thermodynamically beneficial at all temperatures. The enthalpy change, ΔH°, exhibited a negative value in this system, providing more evidence of the exothermic character of the adsorption process. The presence of negative entropy values provides evidence for the potential occurrence of advantageous adsorption [72].

Table 4. Thermodynamic coefficients for methylene blue MB

Sample	- Δ G^0(K J/mol)			- ΔH^0 (K J/mol)	- ΔS^0 (J/mol .K^0)
	303	313	323		
PS	3.27	3.22	3.13	5.46	7.20
SPS	4.19	4.13	4.09	5.65	4.85

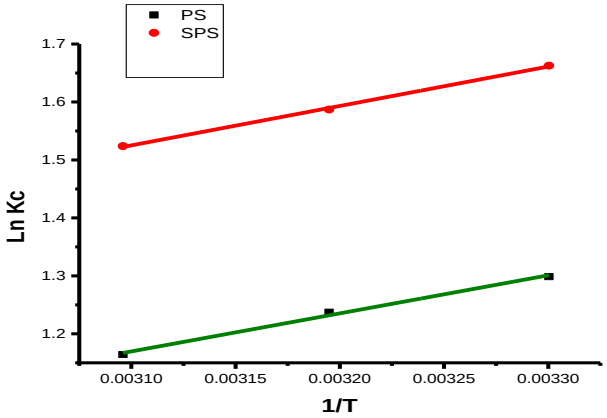

Figure 12: Thermodynamic coefficients for methylene blue MB (PS, and SPS).

3.3.9 Ionic strength

An investigation was conducted to examine the influence of ionic strength on the removal of MB dye from a water-based solution utilizing PS, and SPS, with the addition of inorganic salts such as NaCl, NaHCO3, and MgCl2. The results are presented in Table 5. The addition of salts to the solution was found to have a minimal effect on the sorption capacity of all the materials. Nevertheless, when the levels of salt concentrations increase, the decline in sorption capacity becomes increasingly noticeable. The cations present in the solution compete with the cationic dye to occupy the binding sites on the surface of the sorbent. In contrast, the presence of anionic chemicals resulted in a decrease in the absorption capacity. This phenomenon can be explained by the abundant presence of anionic species, such as chloride ions (Cl-), bicarbonate ions (HCO3-), and sulfate ions (SO4-2), in close proximity to the cationic dye molecules. These anionic species hinder the attachment of the dye molecules to the active sites on the surface of the adsorbent material.

Table 5. effect of Ionic strength on the adsorption of MB by PS, and SPS.

Ionic strength	Concentration (M)	Removal%	
		PS	SPS
NaCl	0.1	25.22	30.87
	0.05	53.19	63.14
	0.01	64.26	65.83
$NaHCO_3$	0.1	17.65	36.59
	0.05	40.47	56.31
	0.01	43.10	59.08
$MgSO_4$	0.1	1.75	2.36
	0.05	12.73	14.63
	0.01	30.72	34.85

3.3.10 Desorption and reusability studies

Desorption is a crucial concern as it enables the retrieval of valuable dye and the recycling of the sorbent in many processes. This study investigated the efficacy of four eluents, namely ethanol, HCl, HNO_3, and NaOH (all at a concentration of 0.1M), in terms of their ability to separate compounds. The findings are displayed in table 6. The highest dye recovery was achieved with HNO3 for all materials (exceeding 94%).

Table 6. Effect of eluent_solution on the desorption process of MB.

Eluent_solution	Desorption%	
	PS	SPS
HNO_3	96.45	95.23
HCl	95.39	94.31
Ethanol	90.03	90.59
NaOH	17.12	17.64

The observed elimination efficiency followed the sequence: NaOH < Ethanol < HCl < HNO_3. The study investigated the impact of three different concentrations of HNO_3 (1 M, 0.5 M, and 0.1 M) on PS, and SPS. The results showed that the concentration of all materials tested was 1 M, as shown in Table 7.

Table 7. Effect concentrations of HNO_3 on the desorption process of MB.

Concentration of HNO_3	Desorption%	
	PS	SPS
1	99.42	99.51
0.5	98.19	96.31
0.1	96.45	95.23

To recycle the given sorbent, a total of five cycles of sorption-desorption tests were performed using 1 M HNO_3 as the eluent. Table 8 contains the results. After each cycle, there was a noticeable decline in the sorption capacity of all sorbents. After undergoing five cycles, the efficiency decline demonstrated substantial enhancement in all materials.

Table 8. Repeated degradation of MB dye on the PS, and SPS

Cycle number	Recovery %	
	PS	SPS
1	99.42	99.51
2	98.26	98.42
3	97.61	98.03
4	96.62	96.69
5	95.63	95.46

3. 3.11 Applications

Actual samples were utilized to assess the effectiveness of PS and SPS in absorbing MB dye under ideal experimental conditions. The samples subjected to analysis included wastewater, seawater sourced from Alexandria City, and tap water obtained from our laboratory at Mansoura University. The analytical data are presented in Table 9. The table displays a decrease in the ability of the examined materials to absorb MB dye, which is attributed to the presence of salts in the actual samples, as demonstrated earlier in the analysis of the influence of ionic strength. Furthermore, it has been found that when the concentration of dye increases, its absorption capacity also increases. Based on the findings, it is justifiable to conclude that the examined materials effectively eliminate MB dye from actual samples with a concentration of 50 ppm or lower.

Table 9. Analytical results of adsorption MB in real water samples using the prepared PS, and SPS at 25, 50, 100ppm of MB

Spiked	PS	SPS
Tap water	(Recovery%)	
25 ppm	88.81	90.23
50 ppm	85.05	89.39
100 ppm	73.76	75.16
Wastewater	(Recovery%)	
25 ppm	86.28	89.61
50 ppm	79.06	80.37
100 ppm	69.84	75.68
Sea water	(Recovery%)	
25 ppm	61.81	66.52
50 ppm	39.29	47.30
100 ppm	33.44	35.63

3.3.12 Plausible Mechanism of adsorption of MB onto the mercerized biosorbents

The adsorption mechanism of MB onto mercerized biosorbents can be understood by examining optical pictures of the biosorbents before and after adsorption, doing BET studies, SEM analysis, EDX analysis, and FTIR analysis of the biosorbents before and after MB adsorption

3.3.12.1. Optical images

Figure 13 (a-d) depicts the optical images of PS, SPS, PS-MB, and SPS-MB, respectively. An evident disparity in the color and shape of the materials is noted, as the samples' color transitions from a pale hue (Fig. 15a) to an even lighter shade following the reaction with NaOH (Fig. 15b). The alteration is substantiated by this shift in color. Moreover, the change in the color of the material (PS, SPS) before and after the adsorption of MB dye is regarded as proof that the dye has been absorbed onto the surface of the material. This is evident from the transformation of color to a dark blue-black shade, as depicted in Figure 15 (c). Figure 15(d) illustrates the concentration of the MB solution at 50 ppm before and after adsorption, as determined from batch tests conducted under the ideal conditions being explored.

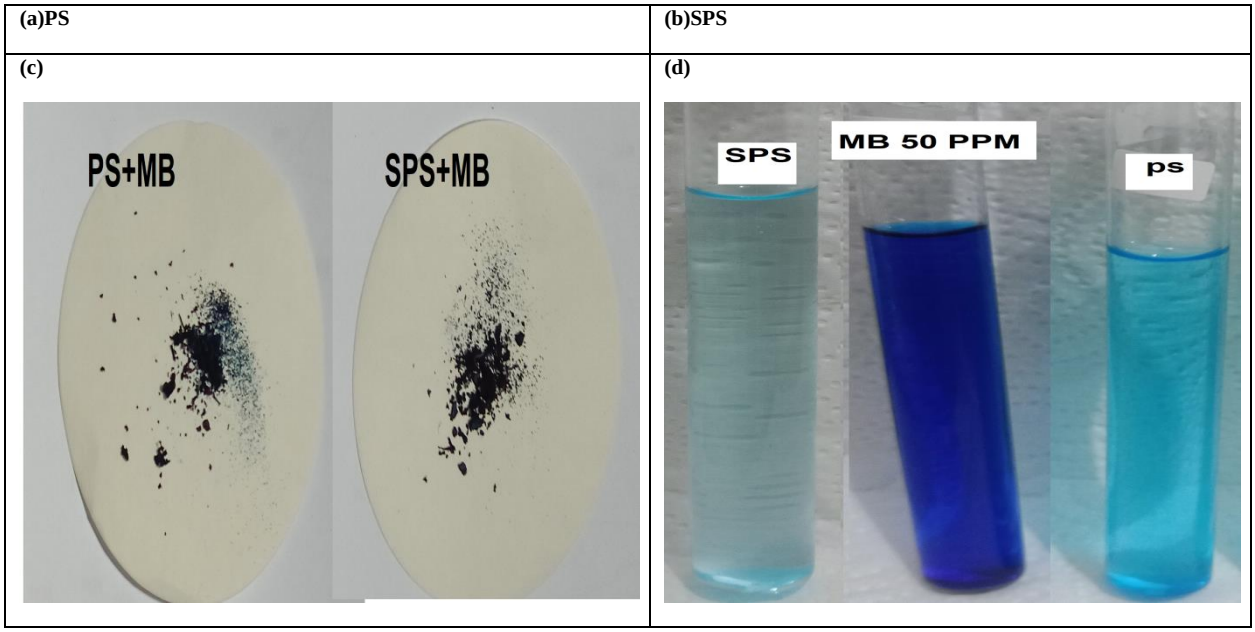

Figure 13 (a-d) depicts the optical images of PS, SPS, PS-MB, and SPS-MB

3.3.12.2. BET studies and N_2 adsorption isotherm

Figure 14 displays the BET and N2 adsorption isotherms for PS, and SPS. The estimated parameters are documented in Table 10. The surface area of PS, and SPS was determined to be 2.0816, and 2.417 m^2/g, respectively. The surface area of SPS exhibited a greater magnitude in comparison to PS. The increase can be ascribed to the reduction in cellulose, hemicellulose, lignin, and other constituents, which is a consequence of the NaOH treatment. The methylene blue molecule has a length of either 13.82 Å [73] or 14.47 Å [74], and a width of approximately 9.5 Å. The length of the molecule is dictated by the precise locations of the chloride ion, which can either be attached to the center sulfur atom or one of the nitrogen atoms on the sides.

Given the size of the methylene blue molecule and the pore sizes of PS, and S PS, it is feasible for methylene blue molecules to enter all of the pores in PS, and SPS.

3.3.12.3. FTIR before and after MB biosorption

The FT-IR spectra depicted in Figure 15 exhibit a notable displacement in the positions of the –OH, C = O, and –C–C– group peaks subsequent to adsorption. This suggests that the binding of MB predominantly takes place at the –OH and C = O sites. The carboxyl group acted as a proton donor, resulting in the creation of the anionic structure of the materials. Hence, the formation of anions due to the existence of -OH and -C=O compounds can be ascribed to their capacity to donate protons and their anionic character, which subsequently attracts MB species. The presence of cations (MB) influences the attraction of anionic formations, showcasing the high adsorption capability of (SPS) towards MB [75]. When SPS are mixed with Methylene Blue (MB), the elongation of the -C-N- bonds in the amine groups becomes apparent, along with a subtle band indicating the bending of the -C-H bonds out of the

plane in the aromatic rings. These observations exhibit typical behaviors of MB [76]. The process of methylation was also found to contribute to the decrease in the broad absorption band of the stretching vibrations of the amino and hydroxyl groups [77].

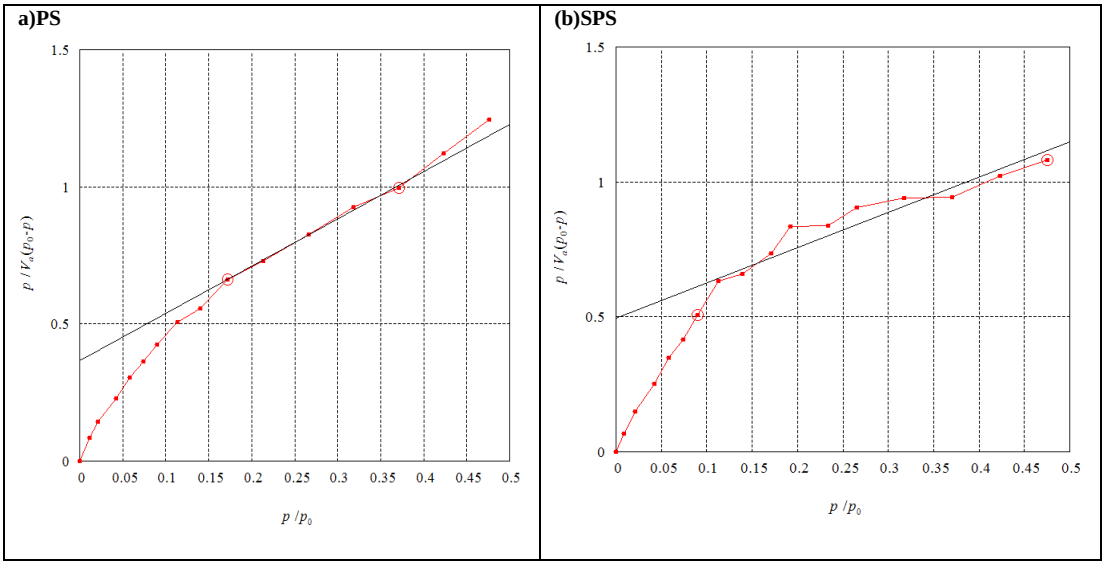

Figure 14: displays the BET plots for (a) PS (b) SPS.

The adsorption of MB onto the PS, and SPS biosorbents can be attributed to various interactions such as pore-filling, electrostatic attraction, π–π, and H-bonding interactions. Figures 16, and 17 depict a schematic illustration of the likely process of MB adsorption onto PS, and SPS biosorbents. The pHpzc values (Table 2) validate the basis of this proposal: PS, and SPS surfaces possess a negative charge, which is enhanced after alkaline modification, hence enhancing the adsorption capacity of the cationic dye (MB).

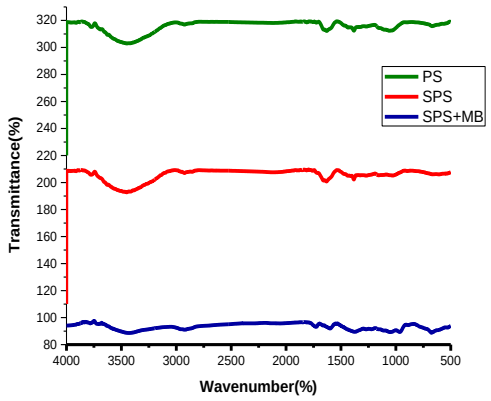

Figure15: IR spectrum before and after adsorption of PS **SPS**, SPS-MB.

The adsorption process of the examined species was anticipated by taking into account the functional groups existing on the surfaces of PS, and SPS. In an alkaline environment, the functional groups that can be found are carbonyl groups (C = O) and hydroxyl (–OH) groups. Within this context, the adsorbents PS, and SPS exhibit the ability to attract and bind MB molecules by electrostatic interactions. The cationic groups (–N+) on the MB molecules interact with the anionic oxygen (CO) on the adsorbents SPS. Additionally, hydrogen bonding is essential in the adsorption process as it enables the interaction between hydrogen atoms on the surface of the adsorbent and nitrogen atoms in the structure of the cationic dye. Figure 18 illustrates the n-π and π-π interactions that take place when the cationic dye (MB) is adsorbed by the adsorbent. The interactions between the electron-donating groups, namely the nitrogen and oxygen groups of the ad-sorbent, and the aromatic rings of the dye are responsible for these interactions [20].

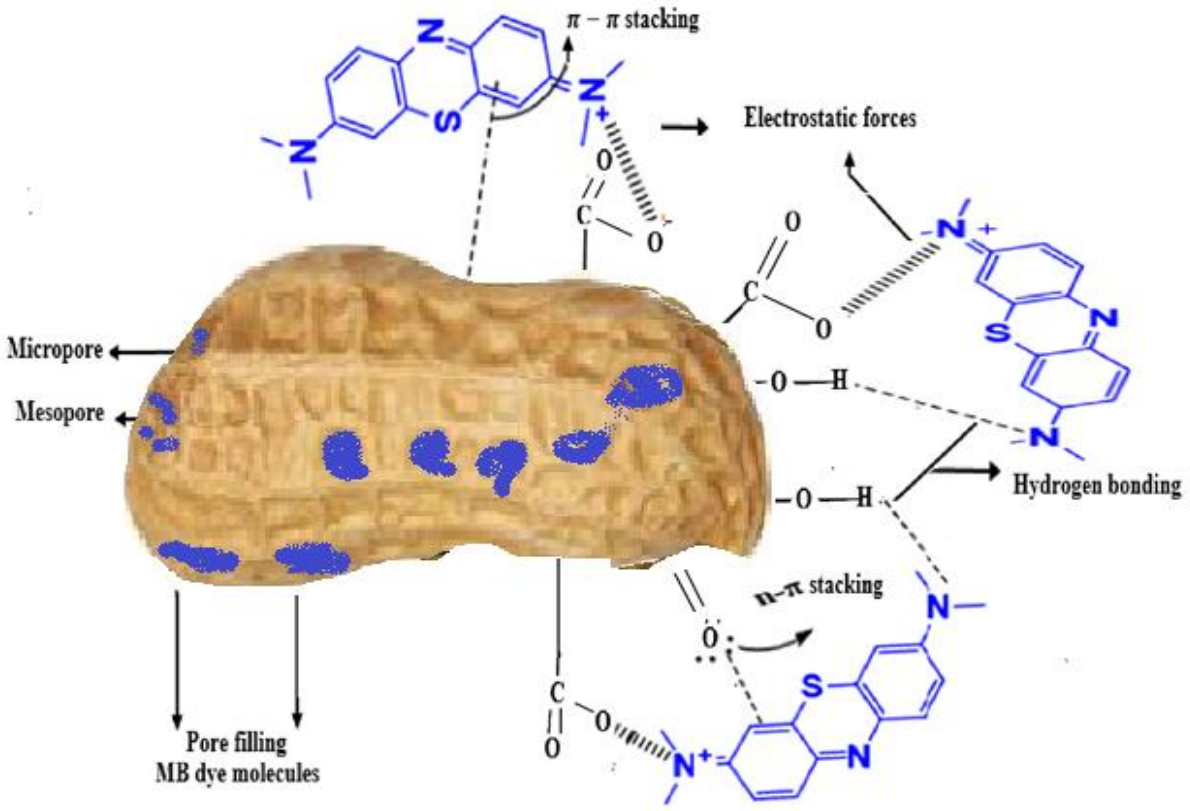

Figure 16: Schematic illustration of the potential MB adsorption process onto SPS.

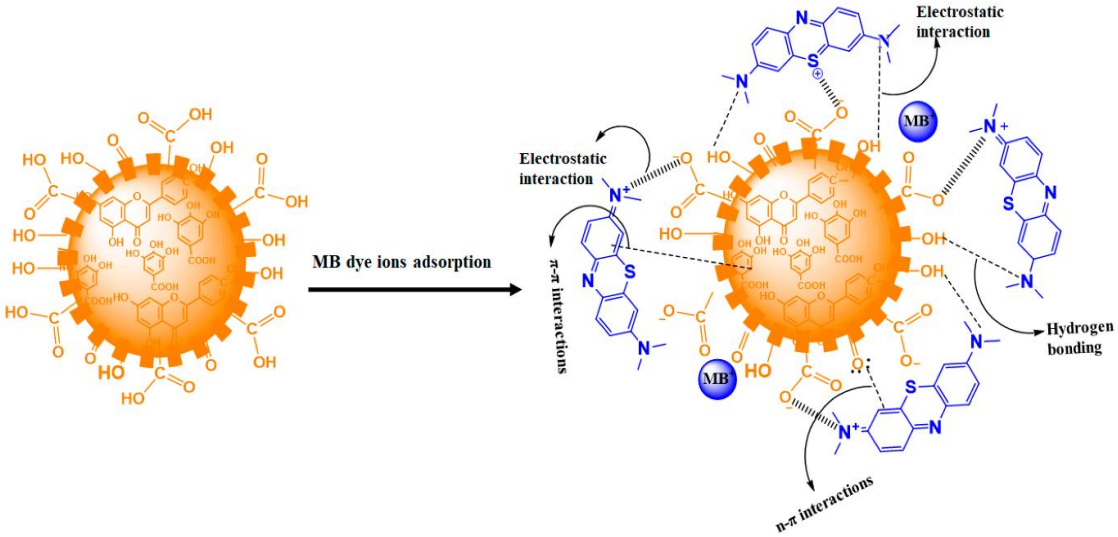

Figure 17: The mechanism of adsorption MB [77].

3.3.13 Dynamic studies

Optimization of the parameters by column test

The study involved optimizing some parameters through the use of a column test. Table 10 displays the factors that were examined and their impact on enhancing the absorption efficiency of MB dye by PS, and SPS

Table 10. Column studies for the maximum removal of MB.

	PS	SPS
Dose effect (g)	With fast flow rate, 10ml, diameter 0.7cm, pH 7.5, 50ppm MB **qe(mg/g)**	
0.1	4.79	4.80
0.15	3.24	3.28
0.2	2.49	2.5
volume effect(ml)	With fast flow rate, 0.1g, diameter 0.7cm, pH7.5, 50ppm MB **Removal%**	
10	94.92	97.37
20	78.27	89.09
30	73.09	78.98
diameter effect(cm)	With fast flow rate, 10ml, 0.1g, pH 7.5, 50ppm MB **Removal%**	
0.7	94.92	97.37
0.9	72.99	88.51
Flow rate effect	With o.1g, 10ml, diameter 0.7cm, pH7.5, 50ppm MB **Removal%**	
fast	94.92	97.37
slow	96.02	99.73

3.3.14. Performance of the prepared biosorbents

Table 11 displays the comparative performance of PS, and SPS in respect to other adsorbents. Comparative studies emphasize the significance of analyzing multiple parameters, including pH, adsorption capacity, equilibration interval, sorbent type, and temperature. According to the investigations, PS, and SPS exhibited a higher capability for MB, as indicated in Table 12.

Table 11. presents the maximum adsorption capacity of several adsorbents for the adsorption of MB.

NO	Adsorbents	Temperature:	pH	Interaction time:	Maximum adsorption capacity (mg/ g)	References
1	Rice straw	35	6	120	32.60	78
2	Walnut shell	25	6	120	51.55	79
3	Moringa oleifera leaf	-	7	90	136.99	73
4	Mango leaf powder	25	7	120	156	80
5	Acacia wood	30 30	7 12	180 180	210.21 280.71	81
6	Onion skin (cold plasma treated)	30	10	150	250	82
7	PS	30	7.5	240	314.24	Present study
8	SPS	30	7.5	240	336.24	Present study

Conclusion

This investigation verifies that peanut shell, which are cost-effective biosorbents, may efficiently adsorb MB from water. The PS, and SPS samples treated with sodium hydroxide (NaOH) have a notable ability to adsorb dye, with absorption capacities were 314.24 mg/g, 336.24 mg/g of PS, and SPS, respectively. The circumstances that yielded the highest absorption of MB were a pH of 7.5, a contact time of 240 minutes, a concentration of 200 ppm, and a temperature of 30°C. The adsorption process can be more accurately characterized by the Langmuir isotherm and exhibits pseudo-second order kinetics, as evidenced by the kinetic investigation. The generated samples demonstrate broad suitability for different water sources, as we have observed their efficient elimination of MB from water matrices with a substantial proportion. Moreover, the does rption experiment showcased the recyclability of the generated samples, as they may be easily reused following the desorption process**.** The subsequent steps of synthesis, cha of PS and SPS and adsorption studies tests are shown in Figure 18

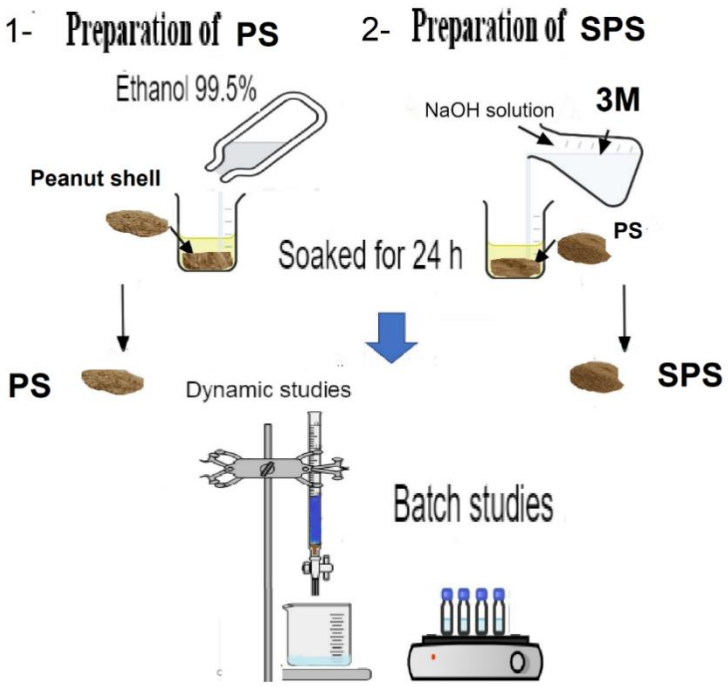

Figure 18: The subsequent steps of synthesis, cha of PS and SPS and adsorption studies tests.

References

1- Akl, M. A., El-Zeny, A. S., Hashem, M. A., El-Gharkawy, E. S. R., & Mostafa, A. G. (2023). Flax fiber based semicarbazide biosorbent for removal of Cr (VI) and Alizarin Red S dye from wastewater. *Scientific Reports*, *13*(1), 8267.

2- Akl, M. A., Hashem, M. A., & Mostafa, A. G. (2022). Synthesis, characterization, antimicrobial and photocatalytic properties of nano-silver-doped flax fibers. *Polymer Bulletin*, 1-33.

3- Ong, S. A., Toorisaka, E., Hirata, M., & Hano, T. (2005). Biodegradation of redox dye Methylene Blue by up-flow anaerobic sludge blanket reactor. *Journal of hazardous materials*, *124*(1-3), 88-94.

4- Kishor, R., Saratale, G. D., Saratale, R. G., Ferreira, L. F. R., Bilal, M., Iqbal, H. M., & Bharagava, R. N. (2021). Efficient degradation and detoxification of methylene blue dye by a newly isolated ligninolytic enzyme producing bacterium Bacillus albus MW407057. *Colloids and Surfaces B: Biointerfaces*, *206*, 111947.

5-Ahmad, A., Khan, N., Giri, B. S., Chowdhary, P., & Chaturvedi, P. (2020). Removal of methylene blue dye using rice husk, cow dung and sludge biochar: Characterization, application, and kinetic studies. *Bioresource technology*, *306*, 123202.

6- Liu, X. J., Li, M. F., & Singh, S. K. (2021). Manganese-modified lignin biochar as adsorbent for removal of methylene blue. *journal of materials research and technology*, *12*, 1434-1445.

7-Bayomie, O. S., Kandeel, H., Shoeib, T., Yang, H., Youssef, N., & El-Sayed, M. M. (2020). Novel approach for effective removal of methylene blue dye from water using fava bean peel waste. *Scientific reports*, *10*(1), 7824.

8-Cheng, J., Zhan, C., Wu, J., Cui, Z., Si, J., Wang, Q., ... & Turng, L. S. (2020). Highly efficient removal of methylene blue dye from an aqueous solution using cellulose acetate nanofibrous memhuskes modified by polydopamine. *ACS omega*, *5*(10), 5389-5400.

9- Santoso, E., Ediati, R., Kusumawati, Y., Bahruji, H., Sulistiono, D. O., & Prasetyoko, D. (2020). Review on recent advances of carbon based adsorbent for methylene blue removal from waste water. *Materials Today Chemistry*, *16*, 100233.

10- Contreras, M., Grande-Tovar, C. D., Vallejo, W., & Chaves-López, C. (2019). Bio-removal of methylene blue from aqueous solution by Galactomyces geotrichum KL20A. *Water*, *11*(2), 282.

11- Jawad, A. H., Abdulhameed, A. S., & Mastuli, M. S. (2020). Acid-factionalized biomass material for methylene blue dye removal: a comprehensive adsorption and mechanism study. *Journal of Taibah University for Science*, *14*(1), 305-313.

12- Cusioli, L. F., Quesada, H. B., Baptista, A. T., Gomes, R. G., & Bergamasco, R. (2020). Soybean hulls as a low-cost biosorbent for removal of methylene blue contaminant. *Environmental Progress & Sustainable Energy*, *39*(2), e13328.

13- Akl, M., & Ahmad, S. A. (2019). Ion flotation and flame atomic absorption spectrophotometric determination of nickel and cobalt in environmental and pharmaceutical samples using a thiosemicarbazone derivative. *Egyptian Journal of Chemistry*, *62*(10), 1917-1931.
14 - Akl, M. A., & Masoud, R. (2018). Flotation and enhanced spectrophotometric determination of uranium (VI) in environmental samples. *Egyptian Journal of Chemistry*, *61*(2), 337-348.
15 - Akl, M. A., El-Mahdy, N. A., & El-Gharkawy, E. S. R. (2022). Design, structural, spectral, DFT and analytical studies of novel nano-palladium schiff base complex. *Scientific Reports*, *12*(1), 17451.
16 - Saleh, M. O., Hashem, M. A., & Akl, M. (2021). Removal of Hg (II) metal ions from environmenta water samples using chemically modified natural sawdust. *Egyptian Journal of Chemistry*, *64*(2), 1027-1034.
17 - Ibrahim, A., El Fawal, G. F., & Akl, M. A. (2019). Methylene blue and crystal violet dyes removal (as a binary system) from aqueous solution using local soil clay: kinetics study and equilibrium isotherms. *Egyptian Journal of Chemistry*, *62*(3), 541-554.
18 - Akl, M. A., El-Zeny, A. S., Hashem, M. A., & El-Gharkawy, E. S. R. (2021). Synthesis, Characterization and Analytical Applications of Chemically Modified Cellulose for Remediation of Environmental Pollutants. *Egyptian Journal of Chemistry*, *64*(7), 3889-3901.
19 - Akl, M. A., El-Zeny, A. S., Ismail, M., Abdalla, M., Abdelgelil, D., & Mostafa, A. G. (2023). Smart guanyl thiosemicarbazide functionalized dialdehyde cellulose for removal of heavy metal ions from aquatic solutions: adsorption characteristics and mechanism study. *Applied Water Science*, *13*(6), 1-18.
20 - Akl, M. A., Mostafa, A. G., Abdelaal, M. Y., & Nour, M. A. K. (2023). Surfactant supported chitosan for efficient removal of Cr (VI) and anionic food stuff dyes from aquatic solutions. *Scientific Reports*, *13*(1), 15786.
21 - Akl, M. A., AL-Rabasi, A., & Molouk, A. F. (2021). Cloud point extraction and FAAS determination of copper (II) at trace level in environmental samples using N-benzamido-N'-benzoylthiocarbamide and CTAB. *Egyptian Journal of Chemistry*, *64*(1), 313-322.
22 - Koe, W. S., Lee, J. W., Chong, W. C., Pang, Y. L., & Sim, L. C. (2020). An overview of photocatalytic degradation: photocatalysts, mechanisms, and development of photocatalytic memhuske. *Environmental Science and Pollution Research*, *27*, 2522-2565.
23 - Kim, S., Yu, M., & Yoon, Y. (2020). Fouling and retention mechanisms of selected cationic and anionic dyes in a Ti3C2T x MXene-ultrafiltration hybrid system. *ACS applied materials & interfaces*, *12*(14), 16557-16565.
24- Mahmoud, M. S., Farah, J. Y., & Farrag, T. E. (2013). Enhanced removal of Methylene Blue by electrocoagulation using iron electrodes. *Egyptian Journal of Petroleum*, *22*(1), 211-216.
25- Lau, Y. Y., Wong, Y. S., Teng, T. T., Morad, N., Rafatullah, M., & Ong, S. A. (2015). Degradation of cationic and anionic dyes in coagulation–flocculation process using bi-functionalized silica hybrid with aluminum-ferric as auxiliary agent. *RSC Advances*, *5*(43), 34206-34215.
26 - García, M. C., Mora, M., Esquivel, D., Foster, J. E., Rodero, A., Jiménez-Sanchidrián, C., & Romero-Salguero, F. J. (2017). Microwave atmospheric pressure plasma jets for wastewater treatment: degradation of methylene blue as a model dye. *Chemosphere*, *180*, 239-246.
27- Banat, F., Al-Asheh, S., & Qtaishat, M. (2005). Treatment of waters colored with methylene blue dye by vacuum membrane distillation. *Desalination*, *174*(1), 87-96.
28- Naresh Yadav, D., Anand Kishore, K., & Saroj, D. (2021). A study on removal of methylene blue dye by photo catalysis integrated with nanofiltration using statistical and experimental approaches. *Environmental Technology*, *42*(19), 2968-2981.
29 - Kong, G., Pang, J., Tang, Y., Fan, L., Sun, H., Wang, R., ... & Sun, D. (2019). Efficient dye nanofiltration of a graphene oxide memhuske via combination with a covalent organic framework by hot pressing. *Journal of Materials Chemistry A*, *7*(42), 24301-24310.
30- Liu, L., He, D., Pan, F., Huang, R., Lin, H., & Zhang, X. (2020). Comparative study on treatment of methylene blue dye wastewater by different internal electrolysis systems and COD removal kinetics, thermodynamics and mechanism. *Chemosphere*, *238*, 124671.
31 - Vakili, M., Rafatullah, M., Salamatinia, B., Abdullah, A. Z., Ibrahim, M. H., Tan, K. B., ... & Amouzgar, P. (2014). Application of chitosan and its derivatives as adsorbents for dye removal from water and wastewater: A review. *Carbohydrate polymers*, *113*, 115-130.
32 - Nayl, A. A., Abd-Elhamid, A. I., Abu-Saied, M. A., El-Shanshory, A. A., Soliman, H. M., Akl, M. A., & Aly, H. F. (2020). A novel method for highly effective removal and determination of binary cationic dyes in aqueous media using a cotton–graphene oxide composite. *RSC advances*, *10*(13), 7791-7802.

33 - Mostafa, A. G., El-Mekabaty, A., Hashem, M. A., & Akl, M. (2021). Selective Separation of Cu (II) from A single Metal Ion Solution by Using O-amino thiophenol-modified flax fiberd. *Egyptian Journal of Chemistry*, *64*(4), 1701-1708.
34 - El-Ghaffar, A., Ahmed, M., Akl, M. A. A., Kamel, A. M., & Hashem, M. S. (2017). Amino acid combined chitosan nanoparticles for controlled release of doxorubicin hydrochloride. *Egyptian Journal of Chemistry*, *60*(4), 507-518.
35 - Akl, M. A., Kamel, A. M., & El-Ghaffar, M. A. A. (2023). Biodegradable functionalized magnetite nanoparticles as binary-targeting carrier for breast carcinoma. *BMC chemistry*, *17*(1), 1-18.
36 - Salleh, M. A. M., Mahmoud, D. K., Karim, W. A. W. A., & Idris, A. (2011). Cationic and anionic dye adsorption by agricultural solid wastes: a comprehensive review. *Desalination*, *280*(1-3), 1-13.
37 - Chowdhury, S., Mishra, R., Saha, P., & Kushwaha, P. (2011). Adsorption thermodynamics, kinetics and isosteric heat of adsorption of malachite green onto chemically modified rice husk. *Desalination*, *265*(1-3), 159-168.
38 – Patil, S., Renukdas, S., & Patel, N. (2011). Removal of methylene blue, a basic dye from aqueous solutions by adsorption using teak tree (Tectona grandis) bark powder. *International journal of environmental sciences*, *1*(5), 711.
39 - Ahmad, H. B., Anwar, T., Ashiq, M. N., Yousaf, M., & Aleem, M. (2011). Comparative studies for the adsorption of remazol blue on rice husk, saw dust and charcoal. *Journal of the Chemical Society of Pakistan*, *33*(4), 449-453.
40 - Salazar-Rabago, J. J., Leyva-Ramos, R., Rivera-Utrilla, J., Ocampo-Perez, R., & Cerino-Cordova, F. J. (2017). Biosorption mechanism of Methylene Blue from aqueous solution onto White Pine (Pinus durangensis) sawdust: Effect of operating conditions. *Sustainable Environment Research*, *27*(1), 32-40.
41 - . Sharma, Y. C., Uma, & Upadhyay, S. N. (2011). An economically viable removal of methylene blue by adsorption on activated carbon prepared from rice husk. *The Canadian Journal of Chemical Engineering*, *89*(2), 377-383.
42 - Alver, E., Metin, A. Ü., & Brouers, F. (2020). Methylene blue adsorption on magnetic alginate/rice husk bio-composite. *International journal of biological macromolecules*, *154*, 104-113.
43 - Gunasekar, V., & Ponnusami, V. (2013). Kinetics, equilibrium, and thermodynamic studies on adsorption of methylene blue by carbonized plant leaf powder. *Journal of chemistry*, *2013*.
44 - Gunasekar, V., Sunil, K., & Ponnusami, V. (2014). Prediction of adsorption kinetic rate constant for removal of Methylene Blue using Teak Leaf Powder. *Asian Journal of Scientific Research*, *7*(3), 284-293.
45- Fiaz, R., Hafeez, M., & Mahmood, R. (2019). Ficcus palmata leaves as a low-cost biosorbent for methylene blue: Thermodynamic and kinetic studies. *Water Environment Research*, *91*(8), 689-699.
46- Dural, M. U., Cavas, L., Papageorgiou, S. K., & Katsaros, F. K. (2011). Methylene blue adsorption on activated carbon prepared from Posidonia oceanica (L.) dead leaves: Kinetics and equilibrium studies. *Chemical Engineering Journal*, *168*(1), 77-85.
47 – Vargas, A. M., Cazetta, A. L., Kunita, M. H., Silva, T. L., & Almeida, V. C. (2011). Adsorption of methylene blue on activated carbon produced from flamboyant pods (Delonix regia): Study of adsorption isotherms and kinetic models. *Chemical Engineering Journal*, *168*(2), 722-730.
48 - Gunasekar, V., & Ponnusami, V. (2013). Kinetics, equilibrium, and thermodynamic studies on adsorption of methylene blue by carbonized plant leaf powder. *Journal of chemistry*, *2013*.
49 - Ong, S., Keng, P., Voon, M., & Lee, S. (2011). Application of durian peel (Durio zibethinus Murray) for removal of methylene blue from aqueous solution. *Asian Journal of Chemistry*, *23*(7), 2898-2902.
50 - Chung, W. J., Shim, J., & Ravindran, B. (2022). Application of wheat husk based biomaterials and nano-catalyst in textile wastewater. *Journal of King Saud University-Science*, *34*(2), 101775.
51 - Pirbazari, A. E., Saberikhah, E., & Kozani, S. H. (2014). Fe3O4–wheat straw: preparation, characterization and its application for methylene blue adsorption. *Water Resources and Industry*, *7*, 23-37.
52 - Jóźwiak, T., Filipkowska, U., & Walczak, P. (2022). The Use of Aminated Wheat Straw for Reactive Black 5 Dye Removal from Aqueous Solutions as a Potential Method of Biomass Valorization. *Energies*, *15*(17), 6257.
53 – Akl, M. A., Hashem, M. A., Ismail, M. A., & Abdelgalil, D. A. (2022). Novel diaminoguanidine functionalized cellulose: synthesis, characterization, adsorption characteristics and application for ICP-AES determination of copper (II), mercury (II), lead (II) and cadmium (II) from aqueous solutions. *BMC chemistry*, *16*(1), 65.
54 – Ouachtak, H., El Guerdaoui, A., Haounati, R., Akhouairi, S., El Haouti, R., Hafid, N., ... & Taha, M. L. (2021). Highly efficient and fast batch adsorption of orange G dye from polluted water using superb organo-montmorillonite: Experimental study and molecular dynamics investigation. *Journal of Molecular Liquids*, *335*, 116560.

55 – Mostafa, A. G., Abd El-Hamid, A. I., & Akl, M. A. (2023). Surfactant-supported organoclay for removal of anionic food dyes in batch and column modes: adsorption characteristics and mechanism study. *Applied Water Science*, *13*(8), 163.
56 – Aryee, A. A., Mpatani, F. M., Kani, A. N., Dovi, E., Han, R., Li, Z., & Qu, L. (2021). A review on functionalized adsorbents based on peanut husk for the sequestration of pollutants in wastewater: Modification methods and adsorption study. *Journal of Cleaner Production*, *310*, 127502.
57 - Akram Khan, M., Guru, S., Padmakaran, P., Mishra, D., Mudgal, M., & Dhakad, S. (2011). Characterisation studies and impact of chemical treatment on mechanical properties of sisal fiber. *Composite Interfaces*, *18*(6), 527-541.
58 - Wirawan, W. A., Choiron, M. A., Siswanto, E., & Widodo, T. D. (2022). Morphology, structure, and mechanical properties of new natural cellulose fiber reinforcement from waru (Hibiscus tiliaceus) bark. *Journal of Natural Fibers*, *19*(15), 12385-12397.
59 - Han, W., & Geng, Y. (2023). Optimization and characterization of cellulose extraction from olive pomace. *Cellulose*, *30*(8), 4889-4903.
60 - Serage, A. A., Mostafa, M. M., & Akl, M. A. (2022). Low Cost Agro-Residue Derived Biosorbents: Synthesis, Characterization and Application for Removal of Lead Ions ffrom Aqueous Solutions. *Egyptian Journal of Chemistry*, *65*(131), 447-461.
61 - Yokota, S., Nishimoto, A., & Kondo, T. (2022). Alkali-activation of cellulose nanofibrils to facilitate surface chemical modification under aqueous conditions. *Journal of Wood Science*, *68*(1), 14.
62 - Thandavamoorthy, R., Devarajan, Y., & Thanappan, S. (2023). Analysis of the characterization of NaOH-treated natural cellulose fibre extracted from banyan aerial roots. *Scientific Reports*, *13*(1), 12579.
63 - Akindoyo, J. O., Pickering, K., Beg, M. D., & Mucalo, M. (2023). Combined digestion and bleaching of New Zealand flax/harakeke fibre and its effects on the mechanical, thermal, and dynamic mechanical properties of poly (lactic) acid matrix composites. *Composites Part A: Applied Science and Manufacturing*, *164*, 107326.
64 - Han, W., & Geng, Y. (2023). Optimization and characterization of cellulose extraction from olive pomace. *Cellulose*, *30*(8), 4889-4903.
65 - Yang, X., Li, L., Zhao, W., Wang, M., Yang, W., Tian, Y., ... & Zhu, X. (2023). Characteristics and Functional Application of Cellulose Fibers Extracted from Cow Dung Wastes. *Materials*, *16*(2), 648.
66 - Segal, L. G. J. M. A., Creely, J. J., Martin Jr, A. E., & Conrad, C. M. (1959). An empirical method for estimating the degree of crystallinity of native cellulose using the X-ray diffractometer. *Textile research journal*, *29*(10), 786-794.
67 - Fathi, B., Foruzanmehr, M., Elkoun, S., & Robert, M. (2019). Novel approach for silane treatment of flax fiber to improve the interfacial adhesion in flax/bio epoxy composites. *Journal of Composite Materials*, *53*(16), 2229-2238.
68 - Vijay, R., Singaravelu, D. L., Vinod, A., Sanjay, M. R., & Siengchin, S. (2019). Characterization of alkali-treated and untreated natural fibers from the stem of parthenium hysterophorus. *Journal of Natural Fibers*.
69 - Khenblouche, A., Bechki, D., Gouamid, M., Charradi, K., Segni, L., Hadjadj, M., & Boughali, S. (2019). Extraction and characterization of cellulose microfibers from Retama raetam stems. *Polímeros*, *29*.
70 – Azadeh, E., Seyed, F., & Ardovan, Y. (2015). Surfactant-modified wheat straw: preparation, characterization and its application for methylene blue adsorption from aqueous solution. *J Chem Eng Process Technol*, *6*, 231.
71 - Do, T. H., Dung, N. Q., Chu, M. N., Van Kiet, D., Ngan, T. T. K., & Van Tan, L. (2021). Study on methylene blue adsorption of activated carbon made from Moringa oleifera leaf. *Materials Today: Proceedings*, *38*, 3405-3413.
72 - Banerjee, S., Chattopadhyaya, M. C., Uma, & Sharma, Y. C. (2014). Adsorption characteristics of modified wheat husk for the removal of a toxic dye, methylene blue, from aqueous solutions. *Journal of Hazardous, Toxic, and Radioactive Waste*, *18*(1), 56-63.
73 - De Souza Macedo, J.; da Costa Júnior, N.B.; Almeida, L.E.; da Silva Vieira, E.F.; Cestari, A.R.; de Fátima Gimenez, I.; Villarreal Carreno, N.L.; Barreto, L.S. Kinetic and calorimetric study of the adsorption of dyes on mesoporous activated carbon prepared from coconut coir dust. J. Colloid Interface Sci. 2006, 298, 515–522
74 - Dotto, G.L.; Santos, J.M.N.; Rodrigues, I.L.; Rosa, R.; Pavan, F.A.; Lima, E.C. Adsorption of methylene blue by ultrasonic surface modified chitin. J. Colloid Interface Sci. 2015, 446, 133–140.
75 - Adelodun, B., Ajibade, F. O., Abdulkadir, T. S., Bakare, H. O., & Choi, K. S. (2020). SWOT analysis of agro-waste based adsorbents for persistent dye pollutants removal from wastewaters. *Environmental Degradation: Causes and Remediation Strategies; Kumar, V., Singh, J., Kumar, P., Eds*, 88-103.
76 - Salazar-Rabago, J. J., Leyva-Ramos, R., Rivera-Utrilla, J., Ocampo-Perez, R., & Cerino-Cordova, F. J. (2017). Biosorption mechanism of Methylene Blue

from aqueous solution onto White Pine (Pinus durangensis) sawdust: Effect of operating conditions. *Sustainable Environment Research*, *27*(1), 32-40.
77 - Dharmalingam, V., Ramasamy, A. K., & Balasuramanian, V. (2011). Chemical modification on reactive dye adsorption capacity of castor seeds. *E-Journal of Chemistry*, *8*(S1), S335-S343.
78 – AL-Shehri, H. S., Alanazi, H. S., Shaykhayn, A. M., ALharbi, L. S., Alnafaei, W. S., Alorabi, A. Q., ... & Alharthi, F. A. (2022). Adsorption of methylene blue by biosorption on alkali-treated solanum incanum: isotherms, equilibrium and mechanism. *Sustainability*, *14*(5), 2644.
79 - Fathy, N. A., El-Shafey, O. I., & Khalil, L. B. (2013). Effectiveness of alkali-acid treatment in enhancement the adsorption capacity for rice straw: the removal of methylene blue dye. *ISRN physical chemistry*, *2013*, 1-15.
80 - Tang, R., Dai, C., Li, C., Liu, W., Gao, S., & Wang, C. (2017). Removal of methylene blue from aqueous solution using agricultural residue walnut shell: equilibrium, kinetic, and thermodynamic studies. *Journal of Chemistry*, *2017*.
81 - Uddin, M. T., Rahman, M. A., Rukanuzzaman, M., & Islam, M. A. (2017). A potential low cost adsorbent for the removal of cationic dyes from aqueous solutions. *Applied Water Science*, *7*, 2831-2842.
82 - Yusop, M. F. M., Ahmad, M. A., Rosli, N. A., & Abd Manaf, M. E. (2021). Adsorption of cationic methylene blue dye using microwave-assisted activated carbon derived from acacia wood: optimization and batch studies. *Arabian Journal of Chemistry*, *14*(6), 103122.
83 - Saka, C., & Sahin, Ö. (2011). Removal of methylene blue from aqueous solutions by using cold plasma-and formaldehyde-treated onion